Tests of Concrete Bridge Columns with Interlocking Spiral Reinforcement

GRANT C. BUCKINGHAM, DAVID I. MCLEAN, AND C. ERNEST NELSON

The behavior of concrete bridge columns incorporating interlocking spirals under flexural, shear, and torsional loadings was investigated experimentally. Tests were performed on approximately 1/5-scale column specimens subjected to increasing levels of cycled inelastic displacements under constant axial load. Rectangular and oval cross sections with either two interlocking spirals or conventional ties were investigated. Variables studied included the performance of interlocking spirals compared to ties, the amount of spiral overlap, and the size of longitudinal bars required in the overlap region to maintain spiral interlock. Column performance was evaluated in terms of lateral load capacity, strength degradation, energy dissipation, and failure mechanisms. Columns with interlocking spirals performed as well or better than columns with ties, despite approximately 50 percent more transverse reinforcement being provided in the tied columns. Test results indicated improved performance when the center-to-center spacing of interlocking spirals was not greater than 0.6 times the spiral diameter. At least four longitudinal bars of approximately the same size as the main longitudinal reinforcement are required in the overlap region to maintain spiral interlock. When adequate longitudinal bars and spiral overlap were provided, the spirals remained interlocked even when loaded to large displacements thus preserving load transfer between the spirals.

Transverse reinforcement in bridge columns normally consists of spiral reinforcement in columns with circular cross sections and tied reinforcement in columns with square or rectangular cross sections. The circular shape of spiral reinforcement is inherently efficient in providing confinement to the concrete core and restraint of longitudinal bar buckling. In contrast, rectangular columns require cross ties or overlapping ties in addition to the perimeter tie to provide adequate confinement and restraint of bar buckling. As a result, tied columns are often more difficult to construct and require larger amounts of transverse reinforcement than columns with spiral reinforcement.

To incorporate the benefits of spiral reinforcement into noncircular columns, the California Department of Transportation (Caltrans) has begun to use interlocking spirals. Although special construction techniques are required for columns with interlocking spirals, the volume of transverse reinforcement is normally less than that for columns with ties. The seismic performance of columns with interlocking spirals may also be superior to that for tied columns. However, the performance of columns with interlocking spirals has not been fully established.

The Caltrans specifications contain provisions for the design of columns with interlocking spirals (*1*). However, most of the design provisions are apparently based on specifications for single spiral columns with circular cross sections, which may not be adequate for interlocking spiral columns. Furthermore, several important design elements are not addressed in the specifications. Additional information on the behavior of columns with interlocking spirals is needed in order to determine specific design requirements.

The objective of this study was to investigate experimentally the behavior of columns incorporating interlocking spiral reinforcement under shear, flexural, and torsional loading. The effects of several design variables on the behavior of columns with interlocking spirals were investigated, including transverse reinforcement requirements, size of longitudinal bars in the interlock zone, flexural detailing of interlocking spirals in rectangular columns, and performance of columns with interlocking spirals compared with columns with ties. Recommendations are made for the design of bridge columns incorporating interlocking spirals as the transverse reinforcement.

PREVIOUS RESEARCH AND CURRENT PRACTICE

Tests of Columns with Interlocking Spirals

The work done by Tanaka and Park is the only information now available on the experimental behavior of interlocking spiral columns (*2*). Tanaka and Park tested three interlocking spiral columns and one tied column under cyclic lateral load and constant axial load. The column specimens were designed to fail in flexure, and each column was detailed for plastic hinging at the base of the column in accordance with the New Zealand Concrete Design Code. Results of the tests showed similar levels of satisfactory performance for the tied column and the interlocking spiral columns, even though the tied column contained approximately 200 percent more transverse reinforcement by volume than the similar interlocking spiral column.

To ensure force transfer between interlocking spirals, Tanaka and Park proposed that at least four longitudinal bars be placed within the interlock region and that the spacing between centers of adjacent spirals be limited to $1.2r_1$, where r_1 is the radius of the spiral reinforcement. The spacing criterion corresponds to a minimum spiral overlap of 25 percent, where the overlap percentage is defined as the depth of the

G. C. Buckingham, U.S. Army Corps of Engineers, Walla Walla, Wash. 99362. D. I. McLean, Department of Civil and Environmental Engineering, Washington State University, Pullman, Wash. 99164. C. E. Nelson, Bridge and Structures Branch, Washington State Department of Transportation, Transportation Building KF-01, Olympia, Wash. 98504.

interlock region divided by the total depth of the transverse reinforcement.

Caltrans Specifications for Interlocking Spirals

Columns with interlocking spirals are widely used in California, but only limited guidance is given for the design of such columns in the Caltrans specifications (*1*). The specifications set the maximum allowable center-to-center spacing of adjacent spirals at "0.75 times the diameter of the cage," or a minimum spiral overlap of 14.3 percent. Caltrans also requires that at least four longitudinal bars be placed in the interlock region. No requirement is given in the specifications for the minimum cross-sectional area of these interlock bars. Special detailing requirements for interlocking spiral columns with rectangular cross sections have been addressed in the Caltrans bridge design manual (*3*). Longitudinal bars are placed in the four corners of the column and outside both points of spiral intersection to minimize strength losses due to spalling in these areas. The unconfined longitudinal bars are tied into the interlocking spiral core of the column using dead-ended anchors.

EXPERIMENTAL TESTING PROGRAM

Test Specimens and Parameters

Experimental tests were conducted on column specimens with both tied and interlocking spiral transverse reinforcement. The main tests were performed on eight approximately 1/5-scale column specimens subjected to cycled inelastic lateral displacements under constant axial load. The selection of specimen details and test parameters was based on areas of design uncertainty and on results obtained from preliminary tests conducted on approximately 1/25-scale specimens.

Parameters investigated in the experimental testing program included the following:

- Variation in spiral overlap percentage,
- Use of small-diameter (nominal) longitudinal reinforcement in the interlock zone,
- Comparison of column performance with ties and interlocking spirals,
- Variations in flexural detailing, and
- Column cross-sectional shape.

Cross sections and reinforcement layout for the specimens investigated in the 1/5-scale study are shown in Figure 1. Details of the 1/5-scale testing program are summarized in Table 1. Additional information on the testing program can be found elsewhere (*4*).

The concrete used for all 1/5-scale specimens was typical of concrete used for bridge column construction. The concrete consisted of Type I/II portland cement, river-gravel coarse aggregate with a maximum size of $\frac{3}{4}$ in., sand, water reducer, and an air-entraining agent. The average compressive strength at the time of testing was approximately 4600 psi. (Conversion factors for this paper are as follows: 1 in. = 25.4 mm, 1 kip = 4.448 kN, 1 in.-kip = 113 N-m, and 1 psi = 0.006895 MPa.)

All reinforcement in the 1/5-scale specimens was Grade 60. The ties and spirals were constructed of No. 2 deformed rebar. The column longitudinal steel consisted of No. 4 rebar in the flexural specimens and No. 5 rebar in the shear and torsion specimens, except for Column 4, which had No. 2 rebar in the interlock zone.

Test Setup and Procedures

The test setup for the 1/5-scale shear and flexure specimens is shown in Figure 2. The footing of the test specimen was anchored to a laboratory strong floor. Lateral load was applied using a 55-kip actuator operated under displacement control. Axial load was applied to the top of the column using a 200-kip jack. An axial load of approximately $0.09 f'_c A_g$ was applied to all specimens except that used in the torsion test, which had no axial load (f'_c is the compressive cylinder strength of the concrete, and A_g is the gross area of the column section). The axial loading system resulted in a variation of the axial load during testing of approximately ± 6 percent. The contribution to total applied moment resulting from displacement of the axial loading system was determined to be negligible.

The determination of the column tip horizontal displacement at first yield (Δ_y) and the loading sequence was similar to the procedures used by Priestley and Park (*5*). To demonstrate the ductility and hysteretic behavior of the test specimens, the specimens were subjected to a simulated seismic loading pattern consisting of increasing multiples of Δ_y. The loading pattern for the flexure specimens consisted of two cycles at displacement ductility levels (i.e., multiple values of Δ_y) of $\mu = \pm 1, \pm 2, \pm 4, \pm 6$, and ± 8, with the exception of Column 2, which was taken to a maximum displacement level of $\mu \approx \pm 7$ because of actuator stroke limitations; μ is the structure displacement ductility factor, or Δ/Δ_y, where Δ is the column tip horizontal displacement. The loading pattern for the shear test specimens was halted at a displacement ductility level $\mu = \pm 4$ because of failure of the specimen and possible instability of the axial load application system.

The specimen for the 1/5-scale combined shear and torsion test was attached to the laboratory strong floor in the same manner as those for the shear and flexure tests. However, the specimen was offset approximately 6 in. in the direction perpendicular to loading to better facilitate the eccentric loading system. Load was applied to the column with the same 55-kip hydraulic actuator described earlier. A loading collar with a steel W-section welded horizontally to one side provided the eccentric connection necessary to produce the desired combined loading effect. The loading sequence used to test Column 8 consisted of two cycles at displacements of $\pm 0.5, \pm 1.0, \pm 1.5, \pm 2.0, \pm 2.5, \pm 3.0$, and ± 3.5 in. Deflections and loads recorded from the actuator were transformed to equivalent rotations and torques using trigonometric relationships.

Strain gauges were used to monitor the strains in the flexural and transverse reinforcement. Linear variable displacement transformers and load cells measured column displace-

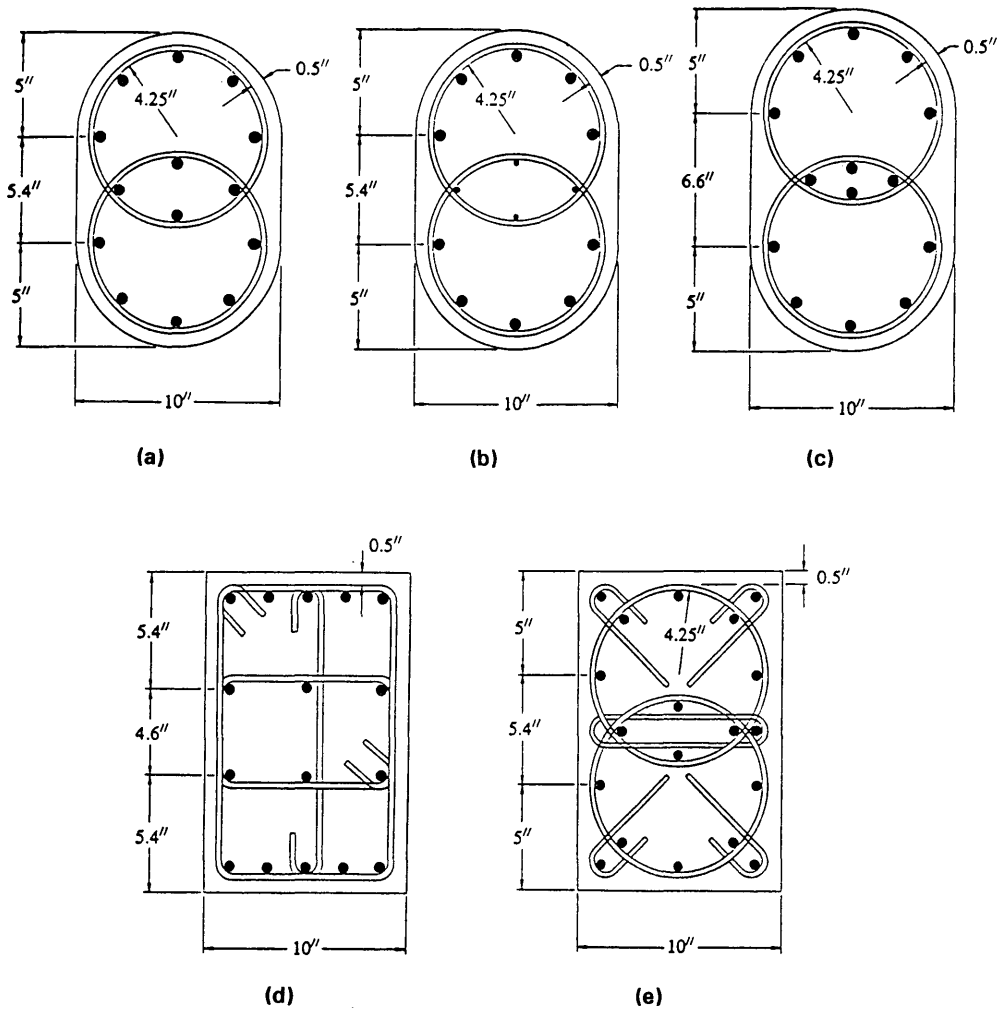

FIGURE 1 Column cross sections and reinforcement layout: *a*, Columns 1, 5, and 8; *b*, Column 4; *c*, Column 3; *d*, Columns 6 and 7; and *e*, Column 2.

TABLE 1 Parameters for 1/5-Scale Specimens

Specimen Number	Type of Loading	Transverse Reinforcement	Spiral/Tie Spacing (in.)	Spiral Overlap (%)	Nominal Interlock Steel	Column Cross-section
1	Shear	Spirals	5.0	25	No	Oval
2	Flexural	Spirals	1.25	25	No	Rectangular
3	Shear	Spirals	5.0	15	No	Oval
4	Shear	Spirals	5.0	25	Yes	Oval
5	Flexural	Spirals	2.5	25	No	Oval
6	Flexural	Ties	2.5	NA	NA	Rectangular
7	Shear	Ties	5.0	NA	NA	Rectangular
8	Torsion	Spirals	5.0	25	No	Oval

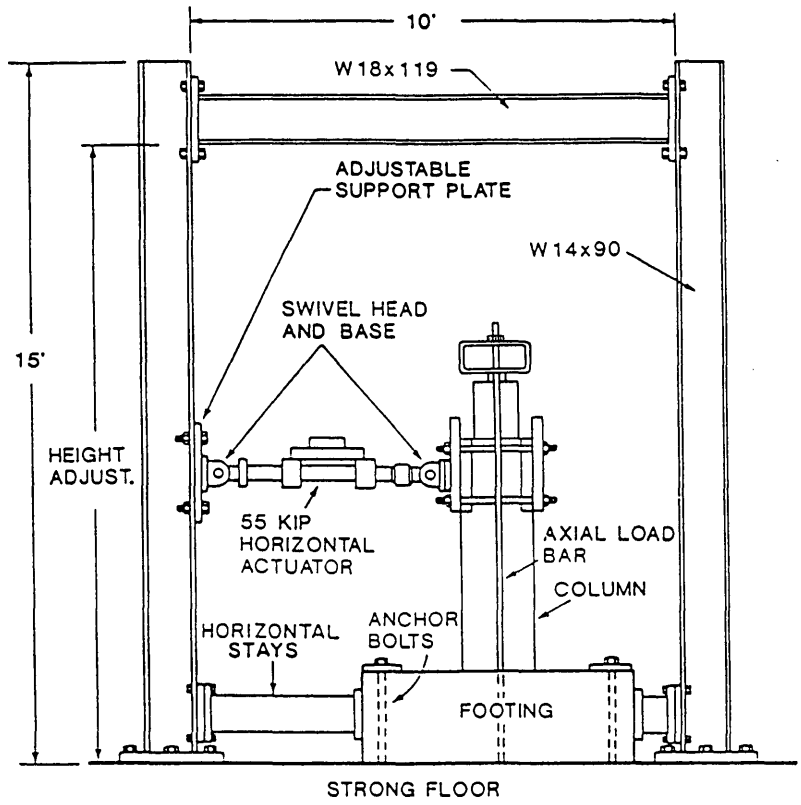

FIGURE 2 Test setup.

ments and applied loads. All data were recorded intermittently during testing.

TEST RESULTS AND DISCUSSION

Shear Tests

General Behavior

Column 1 was an interlocking spiral column with the minimum overlap percentage of 25 recommended by Tanaka and Park (*2*) and full-size longitudinal bars in the interlock zone. Test results from this specimen were used as a guideline for comparison with the other shear tests. Initial cracking occurred at a lateral load of approximately 20 kips. An x-crack pattern typical of shear deficient reinforced concrete columns under cycled inelastic displacements formed at $\mu = \pm 1$, and crack widths increased at $\mu = \pm 2$. Cracking in the specimen eventually led to spalling of the cover concrete and internal fragmentation of the core at $\mu = \pm 4$. The load-displacement curve for Column 1 is shown in Figure 3. The load-carrying capacity of the specimen remains virtually constant at $\mu = \pm 1$ and displays a small decrease at $\mu = \pm 2$. However, severe degradations in lateral load capacity corresponding to the physical damage mentioned earlier are apparent at $\mu = \pm 4$.

Column 4 was designed in the same manner as Column 1 with the exception of the smaller longitudinal bars (No. 2 rebar) in the interlock zone. The initial cracking load for Column 4 was approximately 22 kips. The x-crack pattern displayed in Column 1 was also apparent in this specimen for displacement levels of $\mu \leq \pm 2$. However, the crack widths in Column 4 were larger than those in Column 1 at $\mu = \pm 2$. Spalling of the cover concrete started early in the $\mu = \pm 4$ cycle and was followed by core fragmentation and straightening of the spiral reinforcement. The two nominal interlock bars on the transverse faces of the column displayed significant amounts of deformation due to tensile forces acting on the spiral reinforcement arising from shear on the column. A posttest photograph of one of the nominal interlock bars is shown in Figure 4. The load-deflection curve for Column 4, shown in Figure 5, reflects the physical behavior described previously. Moderate degradation occurs for $\mu \leq \pm 2$, followed by severe degradation at $\mu = \pm 4$ due to core fragmentation and longitudinal reinforcement damage.

Column 3 was constructed with an overlap percentage of 15 to examine the minimum overlap of 14.3 percent recommended by Caltrans (*1*). All of the longitudinal bars in the interlock zone were the same size as the bars used in the rest of the specimen. The initial cracking load and crack pattern exhibited in this specimen were similar to those described for Columns 1 and 4. However, crack widths in Column 3 at $\mu = \pm 2$, shown in Figure 6, were significantly larger than those encountered in the previous two tests at the same level of displacement. Spalling of cover concrete in this specimen commenced in the latter stages of the $\mu = \pm 2$ cycle and continued into the final two cycles at $\mu = \pm 4$. Rupture of the spiral reinforcement, shown in Figure 7, occurred on the first cycle to $\mu = +4$ at approximately 93 percent of full cycle displacement. The load-deflection plot for Column 3 is shown in Figure 8. Decreases in the load-carrying capacity of the column are detectable at every level of displacement ductility past the

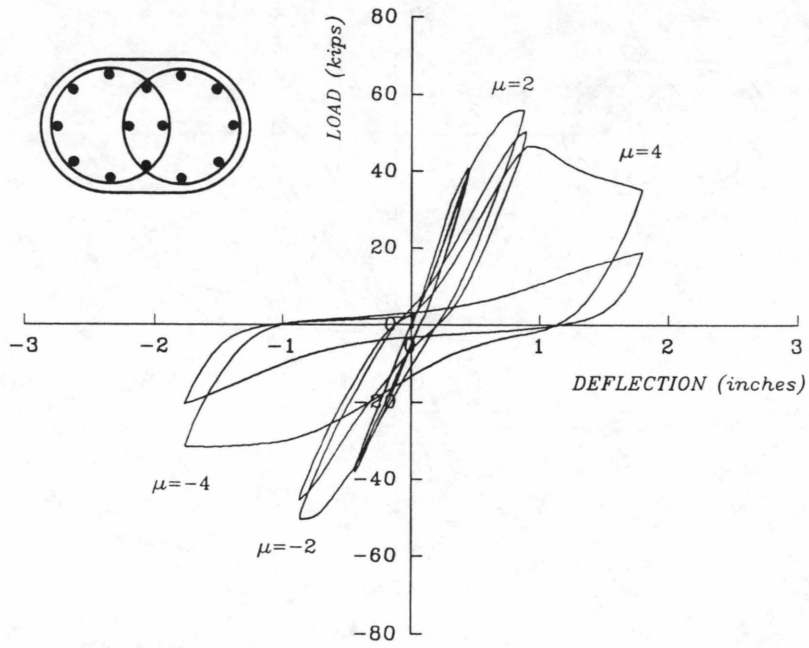

FIGURE 3 Load-displacement curves for shear test, Column 1; Δ_y = 0.45 in.

first cycle to $\mu = +2$. The fracture point of the spiral reinforcement is indicated by the drop in lateral load on the first cycle to $\mu = +4$.

Rectangular ties and cross ties were used as transverse reinforcement in Column 7 to compare the performance of a conventionally reinforced column with one using the interlocking spiral detail (Column 1). A modified testing procedure was used for Column 7 because of limitations encountered in the capacity of the testing equipment. The first two cycles at $\mu = \pm 1$ were accomplished without any alterations to the testing procedure or equipment. However, the load required to attain a displacement corresponding to $\mu = \pm 2$ was beyond the range of the 55-kip hydraulic actuator. After two failed attempts to reach $\mu = +2$ with normal testing procedures, the specimen was relieved of all axial load and cycled manually to produce strength deterioration until the desired displace-

FIGURE 4 Nominal interlock bar in Column 4.

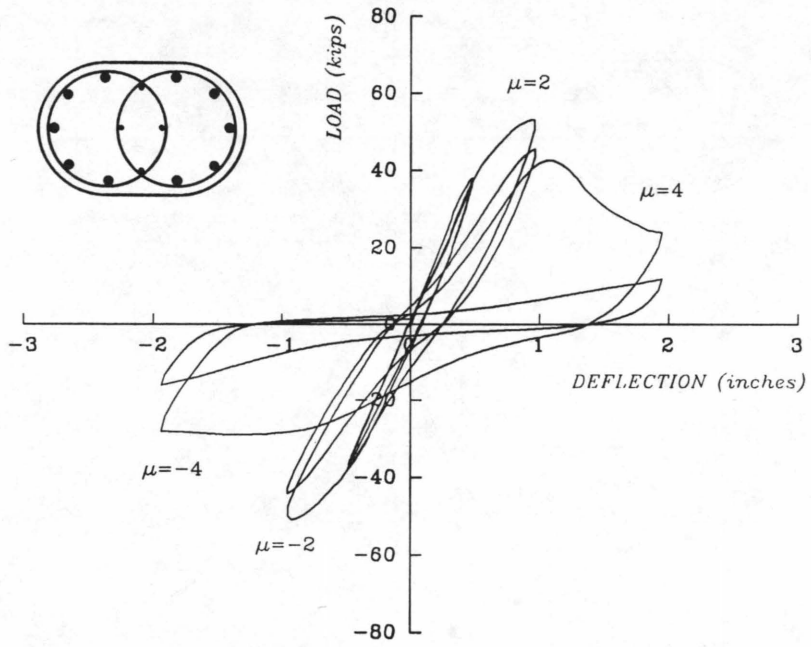

FIGURE 5 Load-displacement curves for shear test, Column 4; Δ_y = 0.495 in.

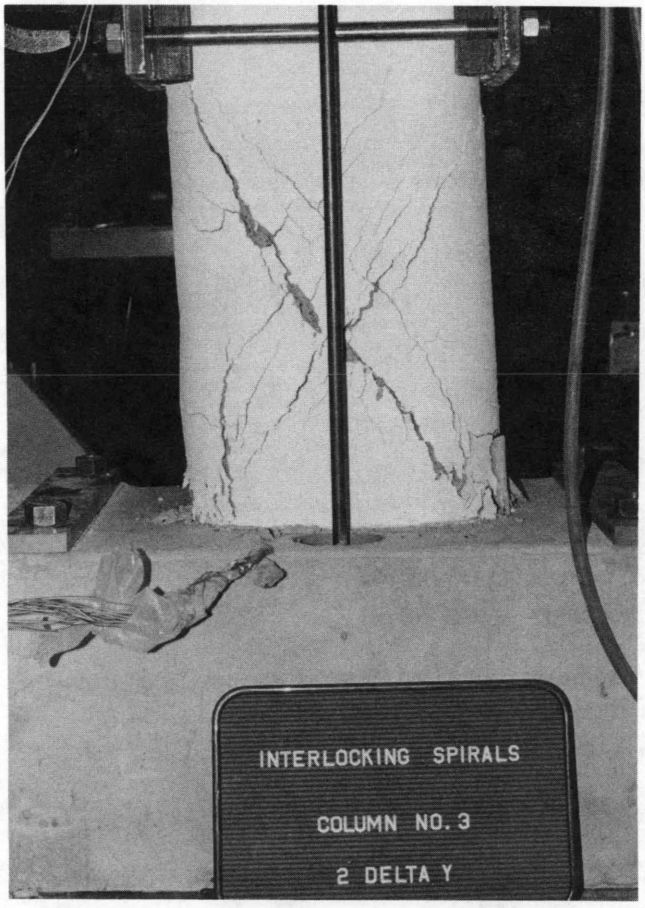

FIGURE 6 Crack patterns in Column 3 at μ = ±2.

ment was obtained. For the cycle to μ = ±4, axial load was returned to the specimen and normal procedures for controlling the lateral load and displacement were resumed. Degradation of Column 7 occurred rapidly in the final two cycles at μ = ±4. The core concrete was reduced to rubble at this stage because of the loss of confinement and possibly also because of the increased number of load cycles imposed on the specimen. A posttest photograph of one of the rectangular ties in Column 7 is shown in Figure 9. The bend angle on the end return has rotated from an original position of 135 degrees to approximately 90 degrees, resulting in a reduction in the confining capability of the tie. Similar damage to the end returns on the internal ties and cross ties also occurred. The load-deflection plot for Column 7 is shown in Figure 10. Although influenced by the increased number of cycles used at μ = ±2, the graph reveals rapid deterioration of the load-carrying capacity of the specimen at μ = ±4, as described earlier. The two sharp drops in load at deflections of approximately 2.0 and 2.5 in. on the first cycle to μ = ±4 correspond to sudden unraveling of rectangular tie end returns.

Comparison of Hysteresis Curves

Comparison of the load-deflection hysteresis curves for the four shear specimens indicates that the reductions in load-carrying capacity for Columns 3 and 4 were greater than the reduction for Column 1 at similar levels of displacement ductility. The hysteresis curves for Column 7 indicate a degradation in load-carrying capacity that is comparable to that in Columns 3 and 4 and is greater than that in Column 1. How-

FIGURE 7 Spiral reinforcement rupture in Column 3.

ever, it is important to note that the testing procedure used for Column 7 was different from that used in the rest of the tests.

Comparison of Calculated and Experimental Strengths

A summary of the experimental and theoretical ultimate shear strengths for the 1/5-scale shear test specimens is given in Table 2. The theoretical shear strengths for the interlocking spiral columns were calculated assuming that the spiral reinforcement was fully effective, and hence the shear contribution of the interlocking spirals was equivalent to that for two spirals. The ratios of experimental to theoretical shear strength for the interlocking spiral columns (Columns 1, 3, and 4) are all within 3 percent of one another. This difference is negligible considering the inconsistent nature of shear failure in reinforced concrete members. The normalized shear

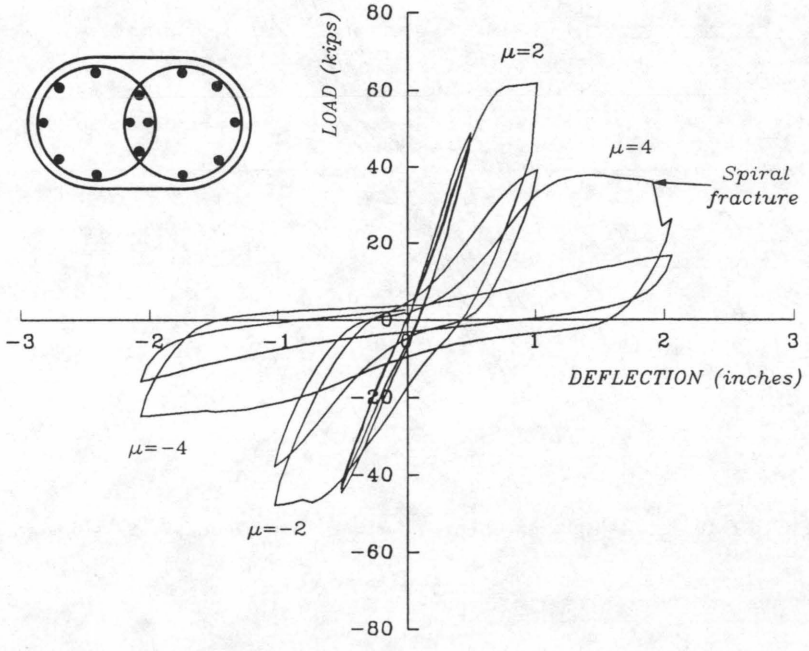

FIGURE 8 Load-displacement curves for shear test, Column 3; Δ_y = 0.52 in.

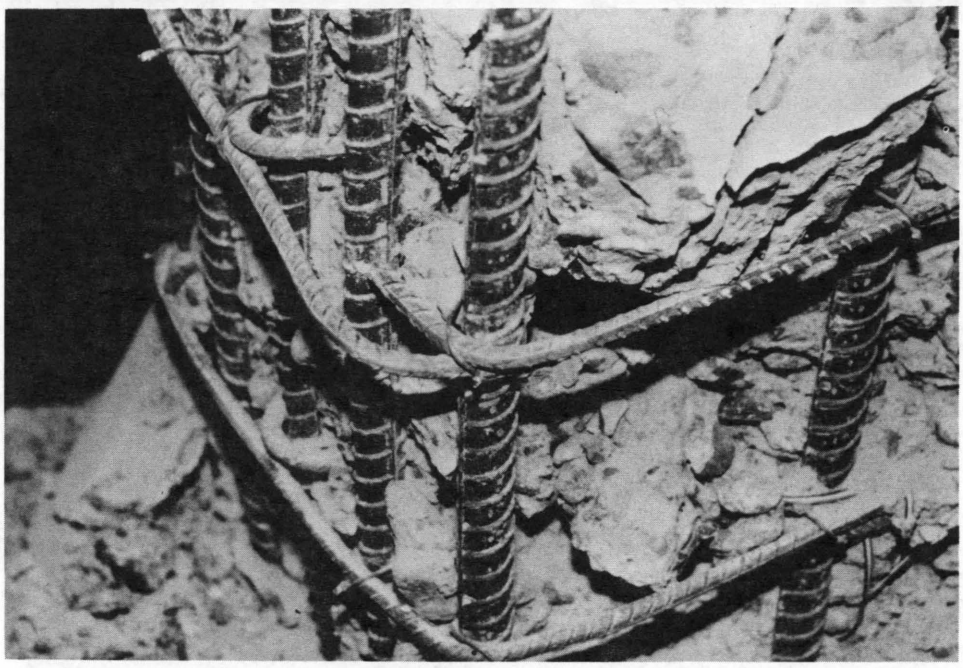

FIGURE 9 Rectangular tie and returns in Column 7.

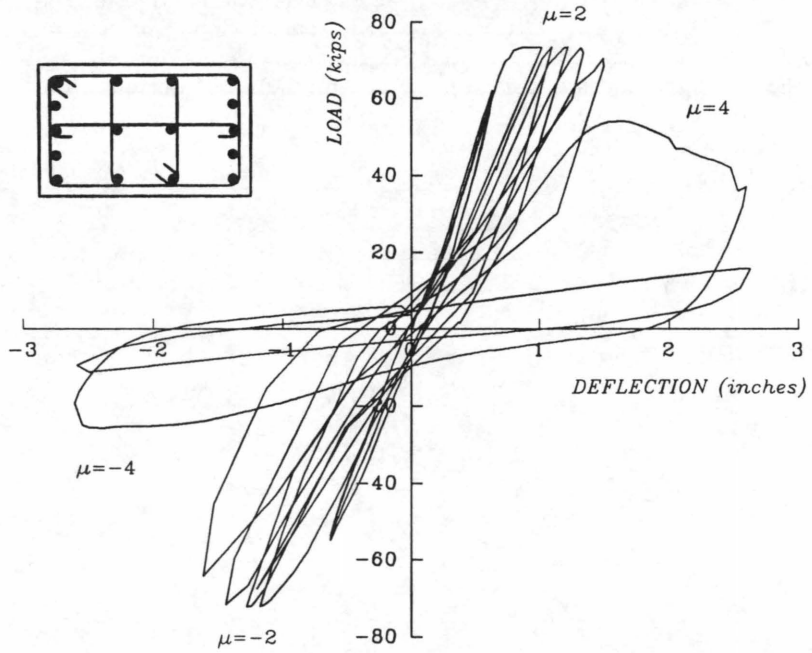

FIGURE 10 Load-displacement curves for shear test, Column 7; Δ_y = 0.66 in.

TABLE 2 Summary of 1/5-Scale Shear Test Results

Specimen Number	V_{test} (kips)	V_n (kips)	$\frac{V_{test}}{V_n}$
1	55.5	41.2	1.347
3	61.9	44.5	1.391
4	53.1	38.5	1.379
7	73.4	53.8	1.364

V_{test} = experimental shear strength
V_n = theoretical shear strength

strength for Column 7 also falls within the range of scatter established by the other shear specimens. The calculated shear strength for Column 7 was determined assuming that all portions of the outer ties, inner ties, and cross ties parallel to the direction of load contributed to shear resistance.

Flexure Tests

General Behavior

The interlocking spiral detail used in Column 5 consisted of a spiral overlap percentage of 25 in an oval-shaped cross section. Flexure cracks initially appeared in Column 5 at a lateral load of approximately 15 kips. At $\mu = \pm 1$, shear and flexure-shear cracks formed along the entire height of the specimen at intervals of 3 to 4 in. Although these cracks persisted throughout the duration of the test, the primary mode of failure in the specimen remained flexural in nature. Crushing of the concrete on the extreme load-bearing faces of the specimen just above the top of the footing occurred at $\mu = \pm 4$ and eventually led to spalling in these areas at $\mu = \pm 6$. On the final cycle to $\mu = +6$, a longitudinal bar buckled outward between two sections of spiral reinforcement. Further cycling of the specimen resulted in fracture of this bar at $\mu = -8$ due to fatigue stress. The load-displacement curve for Column 5 is shown in Figure 11. Except for the sharp drop in lateral load at the point of longitudinal bar fracture, the load-carrying capacity of the specimen remains nearly constant throughout the test.

Column 6 represented a conventionally designed reinforced concrete column with rectangular ties and cross ties used as transverse reinforcement. The initial cracking load for Column 6 was approximately 13 kips. Crack patterns and crack development for this specimen were similar to those in Column 5 for $\mu \leq \pm 2$. Spalling of the cover concrete on both of the extreme compression faces began at $\mu = \pm 4$ because of minor buckling of the longitudinal reinforcement. The lack of confinement from the rectangular ties and cross ties led to severe buckling of the longitudinal reinforcement and unraveling of tie and cross-tie end returns at $\mu = \pm 6$, as shown in Figure 12. Continued cycling through $\mu = \pm 8$ resulted in the fracture of 5 of the 10 longitudinal reinforcing bars concentrated on each of the short faces of the column. The load-deflection plot for Column 6 is shown in Figure 13. The load-carrying capacity of the specimen remains stable for $\mu \leq \pm 6$, then drops significantly at $\mu = \pm 8$ because of fracture of the longitudinal reinforcement.

Column 2 was constructed to investigate a reinforcing detail used for interlocking spiral columns enclosed in rectangular concrete cross sections. The cracking pattern in Column 2 for $\mu \leq \pm 2$ was similar to that described for Column 5. Deterioration of the cover concrete began at $\mu = \pm 4$, along with moderate buckling of the four unconfined corner longitudinal bars. Cycles to $\mu = \pm 6$ and $\mu \approx \pm 7$ led to the fracture of

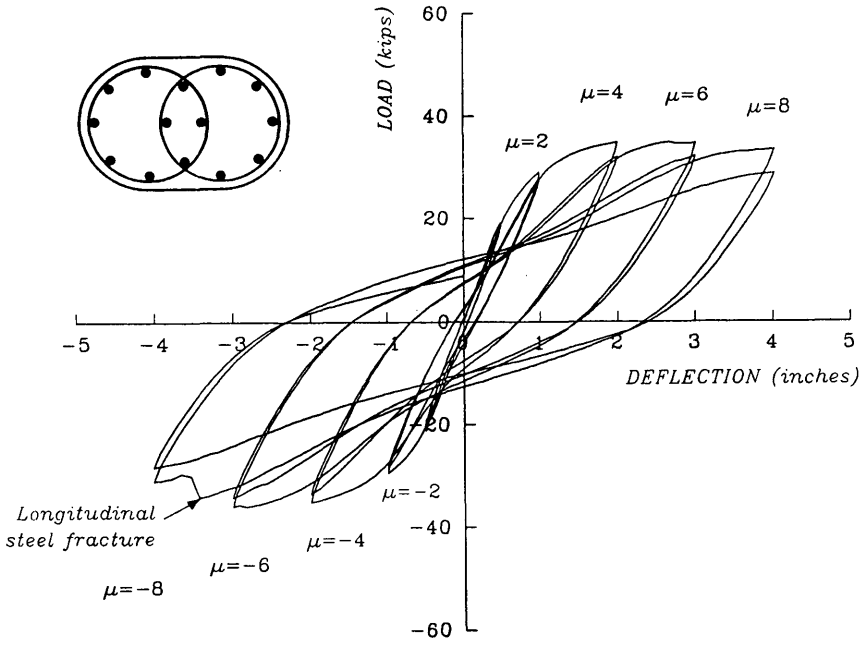

FIGURE 11 Load-displacement curves for flexural test, Column 5; Δ_y = 0.51 in.

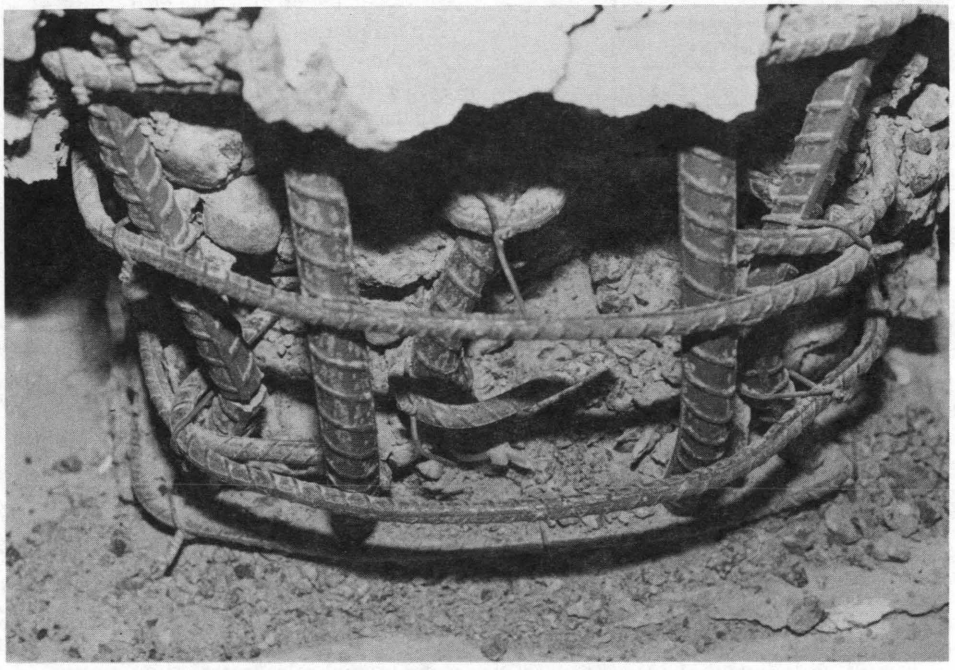

FIGURE 12 Buckling of longitudinal reinforcement in Column 6.

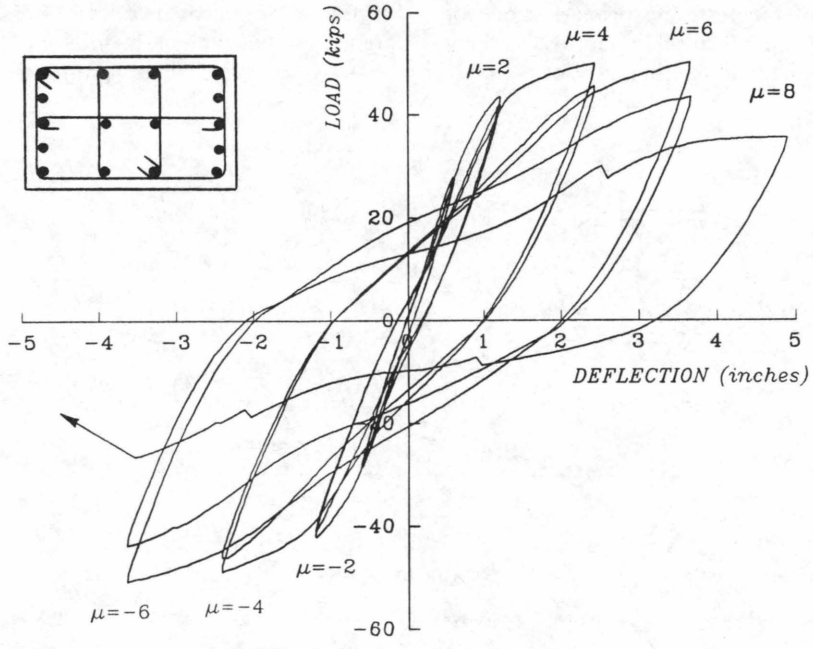

FIGURE 13 Load-displacement curves for flexural test, Column 6; Δ_y = 0.62 in.

all four unconfined corner bars, moderate buckling of the confined longitudinal bar on the extreme bending face, and necking of the spiral reinforcement. The load-deflection plot for Column 2 is shown in Figure 14. The load-carrying capacity of the specimen shows little degradation through $\mu = \pm 4$, then drops sharply during loading to $\mu = \pm 6$ and $\mu \approx \pm 7$ because of longitudinal bar fracture.

Comparison of Hysteresis Curves

Comparison of the load-deflection hysteresis curves for the three flexure specimens indicates that Column 5 maintained a higher percentage of peak load than Columns 6 and 2 at similar levels of displacement ductility. The degradation in load-carrying capacity for Column 2 from $\mu = +4$ to $\mu \approx +7$ is primarily the result of unconfined longitudinal bar fracture.

Comparison of Calculated and Experimental Strengths

A summary of the calculated (using strain compatibility) and experimental ultimate strengths for the 1/5-scale flexure specimens is shown in Table 3. Ratios of experimental and theoretical flexural strength for Columns 2, 5, and 6 display a maximum difference of less than 4 percent.

Combined Shear and Torsion Test

General Behavior

Column 8 was an exact replica of Column 1, with an overlap percentage of 25 and an oval-shaped cross section. The purpose of this test was to investigate the ultimate state behavior of an interlocking spiral column under combined shear and torsional load. Initial cracking in Column 8 occurred at a torsional load of approximately 110 in.-kips. A spiral cracking pattern was exhibited in the specimen and was typical of cracking in reinforced concrete members under combined shear and torsional load. Cracking became more severe at $\Delta = \pm 1.0$ in. (approximately ± 2.88-degree rotation) and was followed by spalling of the cover concrete at $\Delta = \pm 1.5$ in. (approximately ± 4.3-degree rotation). Additional cycles resulted in straightening of the spiral reinforcement around the longitudinal bars and some internal cracking of the concrete core.

The torque-twist curve for Column 8 is shown in Figure 15. The data displayed in the graph include corrections for rotations in the loading collar and actuator and translations parallel and perpendicular to the plane of the reaction frame. The most prominent characteristic depicted in this graph is the difference in specimen degradation at positive and negative values of rotation. A possible explanation for this phenomenon is the fact that spiral reinforcement tends to tighten around the concrete core when twisted in one direction and separate from the core when twisted in the opposite direction.

Interaction Curve for Shear and Torsion

A graph displaying the results from Column 8 with respect to shear and torsion interaction is shown in Figure 16, in which T_{test} is theoretical torsional strength and T_n is experimental torsional strength. The procedure used for calculating the shear strength of Column 8 was the same as that used for the shear test specimens. The torsional strength for Column 8 was calculated using the procedures in ACI 318-89 for rectangular

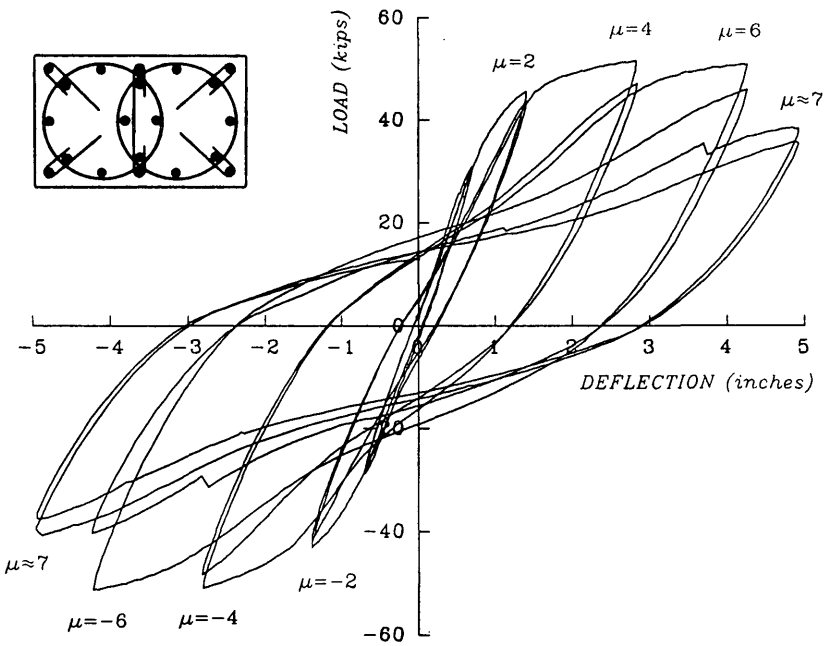

FIGURE 14 Load-displacement curves for flexural test, Column 2; Δ_y = 0.72 in.

TABLE 3 Summary of 1/5-Scale Flexural Test Results

Specimen Number	M_{test} (in.-kips)	M_n (in.-kips)	$\frac{M_{test}}{M_n}$
2	2,477	1,913	1.295
5	1,723	1,291	1.335
6	2,438	1,824	1.337

M_{test} = experimental flexural strength
M_n = theoretical flexural strength

beams. With respect to the shear and torsional strengths, it can be seen in the graph that most of the load applied to Column 8 was torsional in nature. The overstrength displayed for Column 8 is approximately 48 percent. The procedures for calculating the torsional strength of the oval column with interlocking spirals, although apparently conservative, are likely to be inexact. Further research is needed on the behavior of interlocking spiral columns subjected to torsional loading.

CONCLUSIONS AND RECOMMENDATIONS

Conclusions

On the basis of the results of this experimental investigation, the following conclusions are made:

1. Specimens constructed with interlocking spirals for transverse reinforcement performed as well as or better than specimens with ties under both shear and flexural loading, even though the specimens reinforced with ties contained 50 percent more transverse reinforcement than the specimens with interlocking spirals. The superior performance of the interlocking spiral detail would be particularly beneficial in earthquake regions.

2. When loaded to failure in shear, the specimen incorporating a spiral overlap of 25 percent (center-to-center spacing of spirals equal to 0.6 times the spiral diameter) demonstrated less strength degradation than the similar specimen incorporating a spiral overlap of 15 percent (center-to-center spacing of spirals equal to 0.75 times the spiral diameter). Failure in the specimen with the 15 percent overlap was caused by rupture of the spiral reinforcement, whereas failure in the specimen with the 25 percent overlap was a result of gradual deterioration of the concrete core of the column.

3. The use of small-diameter (nominal) longitudinal bars in the interlock region resulted in higher degradation when compared with the similar specimen with the same size of longitudinal bars in the interlock region as that used for the main column reinforcement. The reduced performance of the specimen using nominal interlock bars was due to separation of the spiral cages resulting from severe deformation of the interlock bars.

4. The shear and flexural capacities of columns with interlocking spirals can be reasonably estimated using current procedures for the design of reinforced concrete structures. The torsional capacity of columns with interlocking spirals can be conservatively predicted using an approach adapted from current design equations for the torsional capacity of rectangular beams.

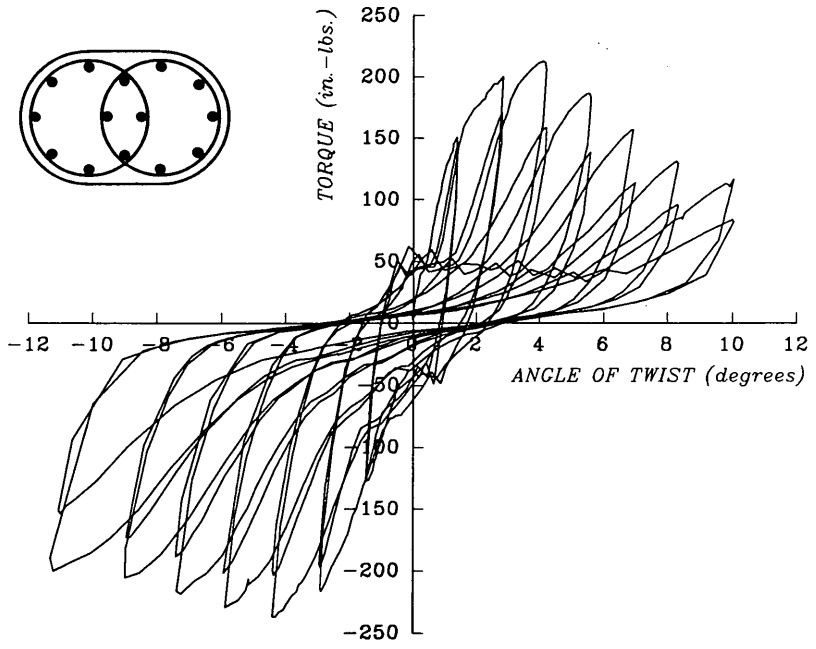

FIGURE 15 Torque-twist curve for Column 8.

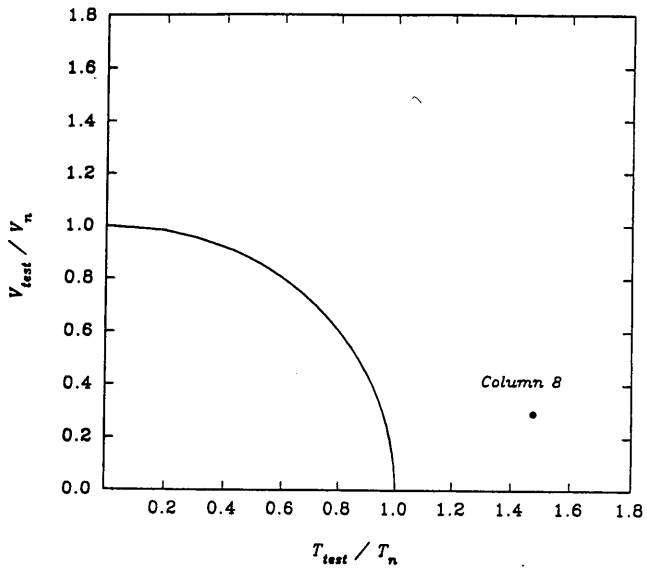

FIGURE 16 Shear-torsion interaction curve for Column 8.

Recommendations

The following recommendations are based on the results of this study and a survey of literature:

1. The center-to-center spacing of adjacent spirals in columns with interlocking spirals should not exceed 0.6 times the diameter of the spiral cage.

2. At least four longitudinal bars of approximately the same size as the main longitudinal reinforcement should be incorporated into the interlock region to prevent the individual spiral cages from separating.

3. Further research is recommended on the torsional behavior of columns with interlocking spirals, particularly in regard to rotation-direction bias resulting in unwinding of the spirals. It is also recommended that the behavior of columns with more than two interlocking spirals be investigated.

REFERENCES

1. *Standard Specifications for Highway Bridges Relating to Seismic Design* (13th ed.). AASHTO, Washington, D.C., 1983. Revisions by the Office of Structures Design, California Department of Transportation, Sacramento, Nov. 1989.
2. H. Tanaka and R. Park. *Effect of Lateral Confining Reinforcement on the Ductile Behavior of Reinforced Concrete Columns*. Report 90-2. Department of Civil Engineering, University of Canterbury, New Zealand, June 1990.
3. *Standard Specifications for Highway Bridges Relating to Seismic Design* (12th ed.). AASHTO, Washington, D.C., 1977. Revisions by the Office of Structures Design, California Department of Transportation, Sacramento, Nov. 1979.
4. G. C. Buckingham. *Seismic Performance of Bridge Columns with Interlocking Spiral Reinforcement*. M.S. thesis. Washington State University, Pullman, 1992.
5. M. J. N. Priestley and R. Park. Strength and Ductility of Concrete Bridge Columns Under Seismic Loading. *ACI Structural Journal*, Vol. 84, No. 1, Jan.–Feb. 1987, pp. 61–76.

Publication of this paper sponsored by Committee on Concrete Bridges.